

Determination of Cross Section for Different Fusion Reactions in Terms of Lattice Effects in Solid State Internal Conversion in Crystalline Palladium Environment

S.N.Hosseini-motlagh¹, M.Shahamiri²

¹ Department of Physics, Shiraz branch Islamic Azad University, Shiraz, Iran

² Sama technical and vocational college, Islamic Azad University, Kazeroon Branch, Kazeroon, Iran

Abstract

In this article, the cross section of different fusion reactions is determined: $D(d,p)T$, $D(d,\gamma)^4\text{He}$, $T(d,n)^4\text{He}$ and $D(p,\gamma)^3\text{He}$ by considering the lattice effect in internal conversion of solid state in palladium environment which is a face-cubic-centered-structured metal. Fusionable particles are solved as sublattice; these particles contribute in fusion reaction in palladium environment. Fusion reaction is generated by flux of incoming fusionable particles. In order to enter the lattice effect in the fusion cross section for above reactions, It need to use The Bloch function for the initial and final state of three-body system. The three-body system consists of the host lattice, sublattice and incident particles. Then the new fusion cross sections are compared with ordinary ones. Finally, the internal conversion coefficient is obtained with regarding the lattice effect. The authors strongly discuss that the lattice effect in solid state internal conversion must be considered until the experimental data of fusion cross section have a good justification with theoretical hypothesis.

Key words: palladium, fusion cross section, crystals, lattice effect

1. Introduction

Nowadays using nuclear energy is very important as a clean source of energy. There are two kinds of nuclear reactions, fusion and fission. Since fusion reaction has less radioactive radiation and the fusion fuels required for these reactions are more sufficiently available in the nature, therefore fusion reactions are important to study.

The ability of palladium to absorb hydrogen was recognized as early as the nineteenth century by Thomas Graham [1]. In 1989, observations of Stanley Pons and Martin Fleischmann about fusion in room temperature gained a lot of attention [2]. After that, the word “cold fusion” was used for Low-Energy Nuclear Reactions (LENR) [3]. All hypotheses about cold fusion failed until 1992 [4-7]. In 1995, many years after Pons and Fleischmann’s separation, Fleischmann continued his researches and published many articles [8]. Although many groups had studied this subject, cold fusion was not accepted officially. The cross section of fusion reactions in metallic environments indicated significant enhancement and its reason have not been proved yet [9]. Meanwhile, one of the controversial hypotheses was electron screening for host particles [10]. In 2007, after many researches, finally cold fusion was accepted officially [11]. Now one of the most controversial issues is cold fusion in metallic crystalline environments [12-14].

In 2002, Peter Kalman and Thomas Keszthelyi studied this problem on different metals. They investigated many different factors to explain the enhancement of fusion cross section. For example,

the electron screening was checked for 29 deuterated metals and 5 deuterated insulators/semiconductors from Periodic Tables. Through these kinds of materials, metals were most convenient. A few prior investigated factors on fusion cross section are: stopping power, thermal motion, channeling, diffusion, conductivity, and crystal structure and electron configuration. None of them could explain and analyses the observed enhancement in crosssection [15-19]. In 2004, these scientists found a reason to explain it, which was called solid state internal conversion [9]. Finally, in 2009, these authors mentioned a metal with its lattice structure and entered the lattice shape of the solid in their internal conversion calculations [20]. Their calculations were performed just for $D(p,\gamma)^3\text{He}$ reaction.

The aim of this work is modification of Peter Kalman and Thomas Keszthelyi studies for other fusion reactions such as $D(d,p)T$, $D(d,\gamma)^4\text{He}$, $T(d,n)^4\text{He}$ of fusion cross section with regarding the lattice effect in solid state internal conversion (LEISSIC). In order to reach into this goal, this article is divided into five general steps. In the first step, we explain how deuterium was solved in palladium lattice as a sublattice. In the second step, the cross section of ordinary state for particular reactions is computed. In the third step, the cross section for three selected reactions in addition to $D(p,\gamma)^3\text{He}$: $D(d,p)T$, $D(d,\gamma)^4\text{He}$, $T(d,n)^4\text{He}$ are calculated. In the fourth step our obtained results of second and third steps are compared. In the five steps, the solid state internal conversion coefficient will be calculated in the presence of lattice effect. Finally, our obtained results are summarized.

2. Method of locating deuterium inside Palladium when deuterium inserted into palladium crystal

Pons and Fleischmann used cathodes including bulk materials (like plates, rods, wires) in their experiments, but here we use ‘atomic cluster’ or nanoparticles. In this article, there is a Double Structure cathode (“DS”-cathode) (figure 1.) [21], DS cathode is made by two parts which is divided into internal cathode (black Pd) and external cathode (Pd plate). Palladium is a transition metal and black palladium is a very fine powder in the form of nanoparticles which is called atomic cluster and it is kept in a vacuum cavity inside palladium plate. In comparison to bulk cathode, DS cathode provides the following applications:

- (a) More than 100 percent of deuterium (means each site of palladium unit cell is possessed by more than one deuterium) immediately are absorbed in internal volume of all black Pd particles because of “diffusion effect” and “atomic cluster effect”.
- (b) The purity degree of deuterium in DS cathode is so high due to “filtering effect” of palladium rod.
- (c) Because of the enhancement pressure of deuterium, the palladium rod obeys from Sieverts law.

In order to carry on the electrolysis in the electrolyte of D_2O/H_2O , this ultra-vacuum cavity inside the Pd rod could easily accommodate highly pure D_2/H_2 gas at over 1000 atoms, which is due to following Sievert law [22, 23]

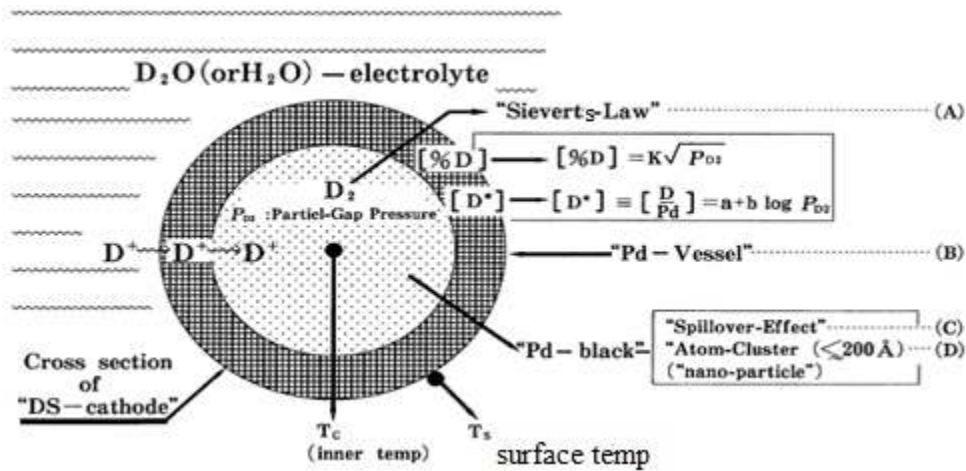


Figure 1: The concept of DS cathode (double structure cathode). (A) High pressure of D_2 gas happens easily inside the DS cathode because of Sievert law. (B) The purity of deuterium in a DS cathode is too high because a palladium rod acts like a filter. (C) Because of the diffusion effect, deuterium immediately distributes on the surface of all black palladium particles uniformly and with a very high density. (D) Nano scale black palladium absorbs many deuteriums with more than 100 percent volume owing to the atomic cluster effect [21].

The FCC structure of solid palladium and octahedral structure, which is sites of deuterium sublattice are respectively presented in Figs 2 and 3. Each palladium unit cell has four palladium atoms distinctively. Thus, each palladium atom in the corners belongs to eight different unit cells in its neighborhood. Since, we have eight atoms in the corners; therefore, each unit cell receives one palladium atom. Every atom is placed on each sides of cube, which is contributed between two neighboring unit cells and because there are six atoms on the sides then each unit cell contains three atoms. One of the palladium unit cells has twenty one sites for deuterium that are located in the sublattice. These twenty one sites are included octahedral, tetrahedral containers and can occupy with twelve deuterium [22].

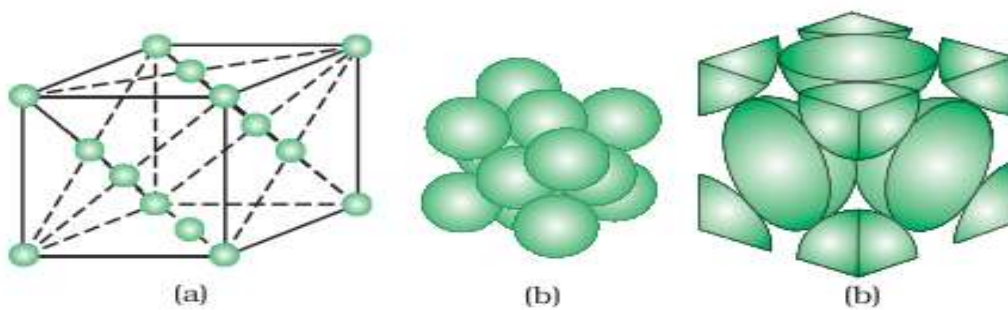


Figure 2: A face-centered cubic palladium unit cell (a). Open structure (b) space filling structure (c) actual portions of atoms belonging to one palladium unit cell.

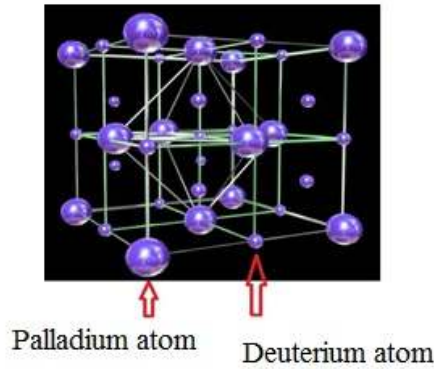


Figure 3: The schematic of the deuterium atom as a sublattice in the palladium unit cell, where big ball and Small ball show palladium site in FCC lattice and deuterium atom in octahedral site in the sublattice, respectively (Image courtesy: J. Dash, J. Freeman, B. Zimmerman) [29].

Among these twenty one sites, eight of the more tetrahedral containers and the rest are octahedral containers. In each tetrahedral container only one deuterium can exist, which is not stable while every octahedral container can accommodate from 1 to 4 deuterium. As a consequence, one unit cell of palladium includes high density of deuterium. This deuterium slice in the palladium unit cell is called pycnodeuterium (Figure 4); “pycno” means high density. Because of high density of deuterium in every palladium unit cell, each unit cell is known as a small cold fusion reactor [23].

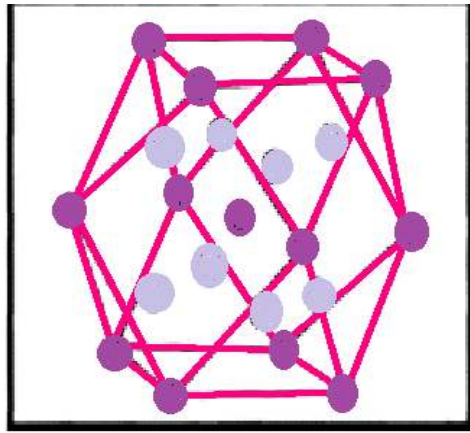


Figure 4: The schematic of the pycnodeuterium slice formed in the palladium unit cell. ● Octahedral container
● Tetrahedral container [23].

3. The scrutiny on the fusion cross section of ordinary state

Whenever the expression “Ordinary State” is appeared means that in determination of cross section, LEISSIC is not counted. Using the extrapolation, the fusion cross section, $\sigma(E)$ of an induced-charged-particle nuclear reaction in the astrophysical energies is given by [15],

$$\sigma(E) = S(E)E^{-1} \exp(-2\pi\eta(E)) \quad (1)$$

Where, $\eta(E)$ and $S(E)$ are the Sommerfeld parameter and the astrophysical S-factor, respectively. It is assumed that the Coulomb potential of the target nucleus and the projectile is the result of bare nuclei. The numerical values of $S(0)$ were calculated completely in the ref [24]. Here, our investigation is performed along the low energy (5-30 eV), the values of $S(0)$ for each reaction is assumed to be constant, which are listed in table 1 for different fusion reactions.

Table 1: The numerical values of astrophysical S-factor for different fusion reactions in ordinary state in low energy

Reactions	$D(p,\gamma)^3\text{He}$	$D(d,p)\text{T}$	$D(d,\gamma)^4\text{He}$	$T(d,n)^4\text{He}$
Astrophysical factor				
$S(0)$ MeV barn	0.2×10^{-6}	0.056	0.054	10

The cross section for ordinary state in terms of incoming particle energy is represented in Fig.5 using Eq.1.

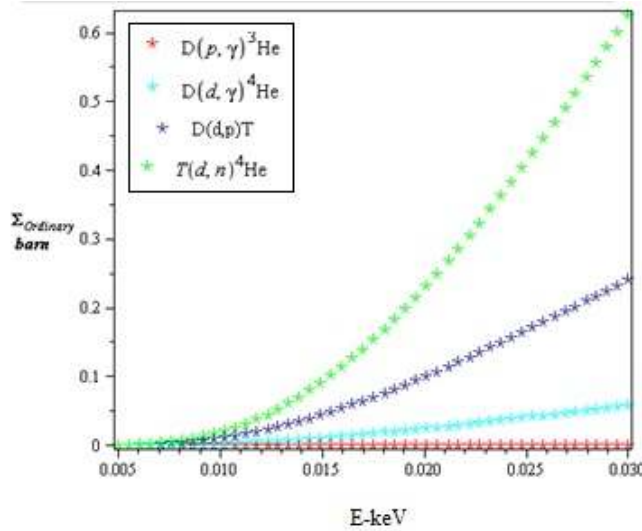


Figure 5: The two dimensional variation of fusion cross section in terms of incoming energy for selected reactions in ordinary state. Each color shows one kind of reaction. Green, dark blue, light blue, and red represent $T(d,n)^4\text{He}$, $D(d,p)\text{T}$, $D(d,\gamma)^4\text{He}$ and $D(p,\gamma)^3\text{He}$ respectively. From this figure we observed that by increasing E , fusion cross section of ordinary state (Σ_{ordinary}) increases too.

4. Determination of fusion cross section with LEISSIC

The electron clouds surrounding the interacting nuclides act as a screening potential and by reducing the Coulomb barrier which is indispensable for performing the fusion reaction. This mechanism, which discussed in section 3 increases the cross section in comparison with the previous state (Ordinary cross section) Eq.1 [15]. The internal conversion (IC) might take place in a solid environment between fusible nuclides and each charged particle in the crystal. IC can involve a

transition between the internal layers of atoms. The particle that transit can be different. In solid state internal conversion (SSIC) there are both electronic and deuterium transition [9]. Therefore, enhancement of cross section in the crystal can be due to IC in extra channels (such as electron and deuterium channels).

4.1. Formulation and importing LEISSIC

Since particles in the crystal are placed in specific sites, we can estimate fusion cross section (FCS) reactions using Block theorem for describing initial and final states of this system (palladium environment). In all formulas subscripts 1, 2 and 3 are respectively pointed at incoming, sublattice and host particles. Also, the state of particles in the lattice is determined by Block function [25]

$$\varphi_{k_{3,i}}(r_3) = \frac{1}{\sqrt{N}} \sum_{l_s} e^{ik_{3,i} \cdot l_s} a_3(r_3 - l_s - u_3(l_s)) \quad (2)$$

Where, r_3 , $k_{3,i}$ and a_3 are respectively introduced host-particle coordinates, a wave vector of the first Brillouan zone of the reciprocal lattice, and the Wannier function. Here, Pd (palladium), d (deuteron) and e (electron) are considered host particles. Lattice site and the displacement of the atom located at lattice site are symbols representing l_s and $u_3(l_s)$. Here N is the number of lattice points. The sublattice particle also is described by the Block function (Eq. 3). Lattice contains N_2 fusionable particles, for palladium system, it is assumed that $N_2 = N$.

$$\varphi_{k_{2,i}}(r_2) = \frac{1}{\sqrt{N_2}} \sum_{l_s} e^{ik_{2,i} \cdot l_s} a_2(r_2 - l_s - u_2(l_s)) \quad (3)$$

Here, a_2 and a_3 are Wannier functions for sublattice and host particles respectively that are defined by equation 4 [20]

$$a_j(x) = \left(\frac{\beta_j^2}{\pi} \right)^{3/4} e^{-\frac{\beta_j^2}{2} x^2} \quad (x = r_2 - l_s), j = 2, 3 \quad (4)$$

In the above formula, $\beta_j = \sqrt{m_j \omega_j / \hbar}$ [26]. The initial state Ψ_i for the three particles that participate in solid state assisted fusion reaction is described by,

$$\Psi_i = \varphi_{k_{2,i}}(r_2) \varphi_{k_{3,i}}(r_3) \varphi_1(r_1 - r_2) \quad (5)$$

Where, $\varphi_1(r_1 - r_2)$ is the Coulomb wave function corresponding to the state of a sublattice and incoming particles. The Coulomb wave function is [20],

$$\varphi_1(r_1 - r_2) = e^{ik_1 \cdot (r_1 - r_2)} \frac{f(k_1, r_1 - r_2)}{\sqrt{V}} \quad (6)$$

V is the volume of normalization, k_1 is the wave vector, r_1 is the coordinate of incoming particles, and f function is defined as the following:

$$f(k_1, x) = e^{-\pi\eta/2} \Gamma(1 + i\eta) {}_1F_1(-i\eta, 1; i[k_1 x - \mathbf{k}_1 \cdot \mathbf{x}]) \quad (7)$$

${}_1F_1$ is the confluent hyper geometric function [27]. η is determined by using the Eqs. 8 and 9 [24].

$$\eta = 0.1575 z_1 z_2 \left(\frac{A}{E}\right)^{1/2} \quad (8)$$

$$A = \frac{A_1 A_2}{A_1 + A_2} (\text{amu}) \quad (9)$$

Where z_1 and z_2 are the charge number of particles 1 and 2 and E is the energy of incoming particles. A_1 and A_2 are the mass of incident and sublattice particles that are measured in amu unit. The final state of this three - body system is,

$$\Psi_f = \psi_f(r_1, r_2) \varphi_f(r_3) F_{Cb}(z_3, z_{12}, v_{3,12}) \quad (10)$$

Where φ_f is a plane wave of wave vector k_3 that is corresponding to an outgoing particle 3.

$$\varphi_f(r_3) = \frac{1}{\sqrt{V}} e^{ik_3 r_3} \quad (11)$$

ψ_f stands for the outgoing fusion product leaving a deuteron lattice point vacancy that the relative coordinate and the center of mass coordinate of the particles of the rest masses m_1 and m_2 are given by: $r = r_1 - r_2$ and $R = m_1 r_1 + m_2 r_2 / m$ respectively, then we have

$$\psi_f(r, R) = \frac{1}{\sqrt{V}} e^{iK.R} \chi(r) \quad (12)$$

Where K and $\chi(r)$ are the wave vector of fusion product and a nuclear wave function, respectively.

$$\chi(r) = \left(\frac{\lambda^2}{\pi}\right)^{3/4} e^{-\lambda^2 r^2 / 2} \quad (13)$$

The Coulomb interaction between host particle and the product of the incident and sublattice reaction are represented as follows by using the Fermi correction;

$$F_{Cb} = \sqrt{2\pi\xi} \frac{e^{-\pi\xi}}{\sqrt{1-e^{-2\pi\xi}}} \quad (14)$$

Here, $\xi = z_3 z_{12} \alpha_f \sqrt{\mu c^2 / 2Q}$ and also α_f is known as the fine structure constant. μ is the reduced mass;

$$\mu = \frac{(m_1 + m_2) m_3}{m_1 + m_2 + m_3} \quad (15)$$

The element of s-matrix that is applied for specifying the cross section of the different fusion reaction is known as,

$$S_{fi} = \frac{2\pi}{i\hbar} \iiint \Psi_f^* \frac{z_1 z_3 e^2}{|r_1 - r_3|} \Psi_i d^3 r_1 d^3 r_2 d^3 r_3 \delta(E/\hbar) \quad (16)$$

with a slight simplification on this integral and using the Hartree-Fok approximation of Coulomb interaction part of the integral, we deliver

$$\frac{z_1 z_3 e^2}{|r_1 - r_3|} = \frac{z_1 z_3 e^2}{2\pi^2} \int d^3 q \frac{1}{q^2} e^{iq \cdot (r_1 - r_2)} \quad (17)$$

Putting the Fourier transform of Eq.13 in Eq.16 and applying the approximation 17 and comparing it with $\langle \sigma v \rangle$ formula, the cross section of fusion reaction between host and target fusible particles is obtained at the following

$$\sigma_2 = C_0 \frac{\exp(-2\pi\eta)}{E} \quad (18)$$

E is the energy of incoming particle and C_0 is determined by,

$$C_0 = |F_{cb}|^2 A_0 k_\mu \left(\frac{\beta_2}{K_Q}\right)^3 \langle |\tilde{\chi}|_{K=K_Q}^2 \rangle_{\Omega_K} \quad (19)$$

with Ω_K denoting the solid angle in the K space, $\beta_2 = \sqrt{m_d \omega / \hbar}$, $A_0 = 128 \alpha_f^3 z_1^3 z_3^2 z_2 m_1 c^2 \sqrt{\pi}$, $K_Q = \sqrt{2\mu c^2 Q} / (\hbar c)$, Q is the energy of the reaction, and $k_\mu = \mu c / \hbar$. The average of nuclear wave function is **determined** by,

$$\langle |\tilde{\chi}|_{K=K_Q}^2 \rangle_{\Omega_K} = \left| \tilde{\chi} \left(\frac{m_2}{m} K \right) \right|^2 = \frac{8\pi^{3/2}}{\lambda^3} e^{-\frac{4K^2}{9\lambda^2}} \quad (20)$$

m_n , **nucleon** mass, ω_n angular frequency of binding energy are **computed** for each reaction separately

$$\lambda = \frac{\sqrt{m_n \omega_n}}{\hbar} \quad (21)$$

$$m_n = m_i + m_{He}, i = d \text{ or } t \quad (22)$$

$$\omega_n = \frac{\text{binding energy of He (MeV)}}{\hbar} \quad (23)$$

The numerical values of m_n , **ω_n , λ** and binding energy of He are calculated and listed in Table.4. Here, C_0 is computed for one d or one Pd. In order to compare C_0 with astrophysical factor (S (0)) in **an** ordinary state, the density of these particles must be accounted. So, we use Eq.24,

$$N C_0 = A \Delta R_h C_1 \quad (24)$$

Such that, N is,

$$N(Pd) = V_{eff} / v_{cell} \quad (25)$$

Where $v_{cell} = d^3 / 4$, $V_{eff} = A \Delta R_h$ and $d = 3.89 \times 10^{-8}$ **cm** is **the lattice** constant

$$N(d) = u V_{eff} / v_{cell} \quad (26)$$

In Eq.23, u is the **proportion** of deuteron to palladium number density. For electron u = 10 which is the number of electron valence in palladium. C_0 contains all the properties of the **lattice**. For comparing the fusion cross section with and without LEISSIC we have to determine the macroscopic cross section:

$$\Sigma = N \sigma_2 \quad (27)$$

5. Results of numerical calculations for each reaction

Tables 2 and 3 can aid in plotting the cross section for all reactions and **comparisons** with the ordinary state. The hypotheses of host, sublattice and incoming particles are expressed for all reactions in this **way: the** host particles are Pd, d, e for Palladium. The sublattice is **considered a** deuterium for all reactions. The incoming particles are proton (p) in $D(p, \gamma)^3\text{He}$, deuterium (d) in $D(d, p)\text{T}$ and $D(d, \gamma)^4\text{He}$ and tritium (t) in $T(d, n)^4\text{He}$. Our calculations for obtaining the cross section for all three **kinds of host particles** are **carried out** by **using the equations**: 14, 15, 19, 20 and 24 and our obtained results are given in tables 2 and 3.

Table 2: Our numerical calculations of necessary quantities for obtaining C_0 for all chosen reactions

Type of Reactions	host particles	$A_0(\text{MeV})$	$\mu(\text{gr})$	$K_Q(\text{cm}^{-1})$	$ \tilde{\chi} _{k=K_Q}^2 (\text{cm}^3)$	ξ
$D(p,\gamma)^3\text{He}$	Pd	175	5.013×10^{-24}	8.91×10^{12}	3.95×10^{-38}	10.755
	d	0.0827	2.005×10^{-24}	5.64×10^{12}	5.13×10^{-38}	0.1477
	e	0.0103	-----	2.78×10^{11}	6.11×10^{-38}	-560382
$D(d,p)\text{T}$	Pd	349	6.686×10^{-24}	8.82×10^{12}	3.15×10^{-38}	14.462
	d	0.165	2.229×10^{-24}	5.09×10^{12}	3.97×10^{-38}	0.181
	e	0.021	-----	2.05×10^{11}	4.45×10^{-38}	-0.0011
$D(d,\gamma)^4\text{He}$	Pd	349	6.686×10^{-24}	7.93×10^{12}	3.69×10^{-38}	16.075
	d	0.165	2.229×10^{-24}	4.58×10^{12}	4.51×10^{-38}	0.202
	e	0.021	-----	1.65×10^{11}	4.98×10^{-38}	-0.0022
$T(d,n)^4\text{He}$	Pd	524	8.35×10^{-24}	2.05×10^{13}	2.89×10^{-39}	5.863
	d	0.248	2.387×10^{-24}	1.10×10^{13}	4.24×10^{-39}	0.09
	e	0.031	-----	8.90×10^{11}	4.30×10^{-38}	-4.228

From the results of Table 2 and Eqs.19 and 24 for different reactions and host particle, we can estimate the required parameters such as C_0 and C_1 which are important for estimating cross section of the fusion reactions.

Table 3: our numerical calculation C_0 and C_1 for different host particle and different reactions

Type of Reactions	host particles	$k_\mu (\text{cm}^{-1})$	$ F_{cb} ^2$	$C_0 (\text{MeV b})$	$C_1 (\text{MeV b})$
$D(p,\gamma)^3\text{He}$	Pd	1.42×10^{14}	3.14×10^{-28}	4.92×10^{-38}	3.36×10^{-24}
	d	0.57×10^{14}	0.61	2.30×10^{-13}	$u \times 15.6$
	e	-----	1	9.10×10^{-13}	6.18×10^2
$D(d,p)\text{T}$	Pd	1.90×10^{14}	3.27×10^{-38}	1.11×10^{-47}	7.53×10^{-34}
	d	0.63×10^{14}	0.5371	1.88×10^{-13}	$u \times 12.78$
	e	-----	1	2.48×10^{-12}	1.687×10^3
$D(d,\gamma)^4\text{He}$	Pd	1.90×10^{14}	7.02×10^{-41}	3.83×10^{-50}	0.26×10^{-35}
	d	0.63×10^{14}	0.4964	2.70×10^{-13}	$u \times 18.35$
	e	-----	1	4.31×10^{-36}	2.93×10^{-21}
$T(d,n)^4\text{He}$	Pd	2.37×10^{14}	4.44×10^{-15}	2.05×10^{-25}	1.39×10^{-12}
	d	0.68×10^{14}	0.7438	4.45×10^{-15}	$u \times 0.3024$
	e	-----	1	1.87×10^{-13}	127.1

Since each palladium unit cell has 4 Pd atoms purely and since we suppose that the number of host and sublattice particles are equal, then we have

$$N_{Pd} = \frac{1}{4} \times 4.22 \times 10^{22} \quad (28)$$

The other quantities such as α , m_n , β_2 and Q which is mentioned before are calculated and numerical results are summarized in Table 4.

Table 4: Required quantities which are calculated for determination of different fusion reactions

Type of Reactions	λ (cm ⁻¹)	β_2 (cm ⁻¹)	Q (MeV)	Binding Energy (MeV)
D(p, γ) ³ He	9×10^{12}	4.81×10^{14}	5.49	7.718
D(d,p)T	10×10^{12}	4.81×10^{14}	4.04	8.482
D(d, γ) ⁴ He	9.63×10^{12}	4.81×10^{14}	3.27	28.3
T(d,n) ⁴ He	21.8×10^{12}	4.81×10^{14}	17.59	28.3

6. Microscopic and macroscopic fusion Cross Section

The fusion cross section of each mentioned reactions is divided into three parts because we have three host particles (Pd,d,e). In addition, there are two kinds of fusion cross section: Microscopic (Mic) (Figure 6, 7) and macroscopic (Mac) (Figure 8, 9) cross sections which are plotted for different reactions by considering different host particles using Eqs.18 and 27 and the values of C_0 in table 3, respectively. The macroscopic cross section is compared with ordinary state (Figs. 10 to 13). We use $\sigma_i a(x, y)b$ and $\Sigma_i a(x, y)b$ to introduce the microscopic and macroscopic fusion cross section, respectively, for each reaction with different host particle where, $i = Pd, d, e$ and $a(x, y)b$ is one of the nuclear reaction. For example, $\sigma_e T(d, n) {}^4He$ is the fusion cross section (FCS) means that the electron host particle for $T(d, n) {}^4He$.

For showing microscopic and macroscopic FCS schematics more clearly, all graphs are divided into seven maximum (seven nations that hold a maximum cross section) (Figs. 6 and 8) and five minimum (five states that have a lower cross section than other seven states) (Figs. 7 and 9) diagrams. In Figs. 6 to 9, “Green” color indicates T(d,n)⁴He reaction, “red”, “dark blue” and “dark pink” indicates D(p, γ)³He, D(d,p)T and D(d, γ)⁴He respectively. We can also realize the kind of host particle by noticing the style of the graph, e.g. “Dash” shows Pd, “Long Dash” electron and “Dash Dot” for deuteron.

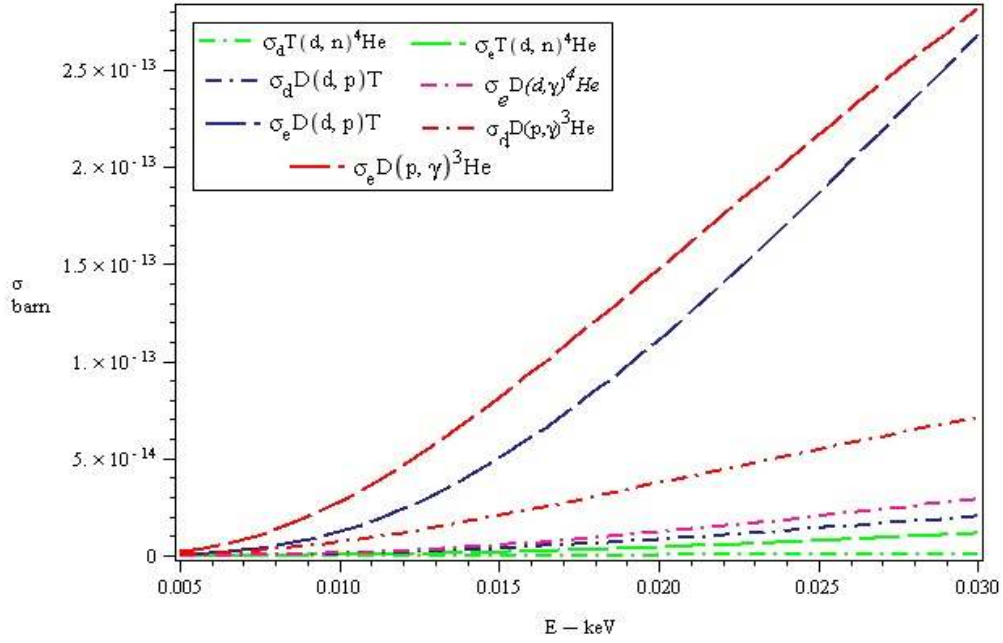


Figure 6: The two dimensional seven maximum modes of microscopic cross section as a function of the incoming particle energy for different host particles and different reactions. The maximum cross sections belong to the electron and deuteron host particles and the best reactions are $D(p, \gamma)^3\text{He}$ and $D(d, p)T$.

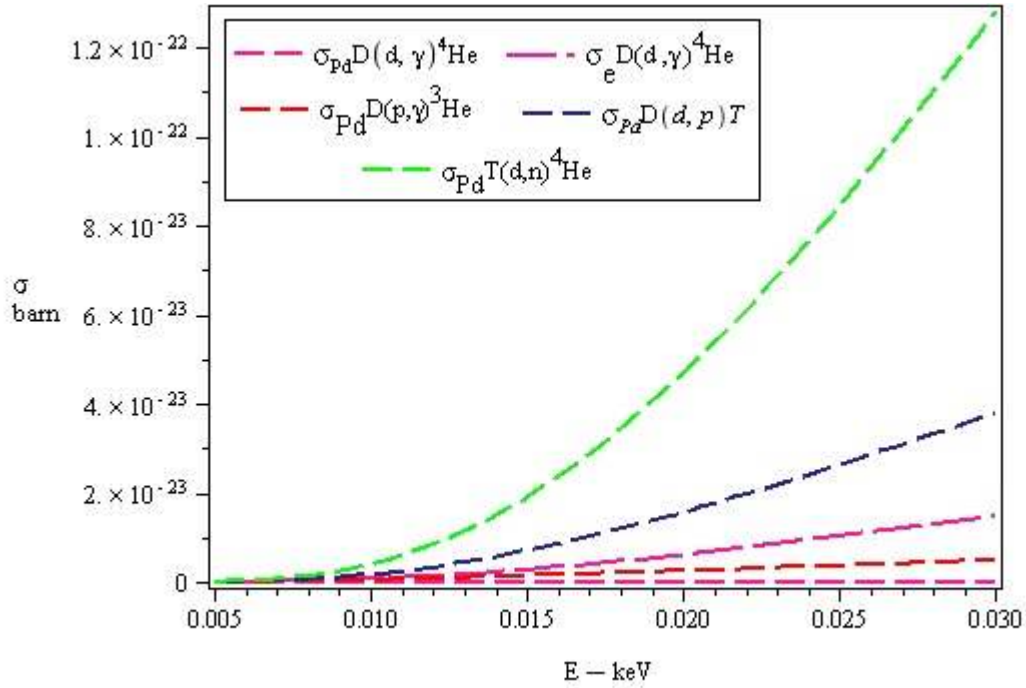


Figure 7: The five minimum microscopic cross sections as a function of the incoming for different host particles and different reactions. In this graph the maximum cross sections belong to palladium host particle for $T(d, n)^4\text{He}$ and $D(d, p)T$.

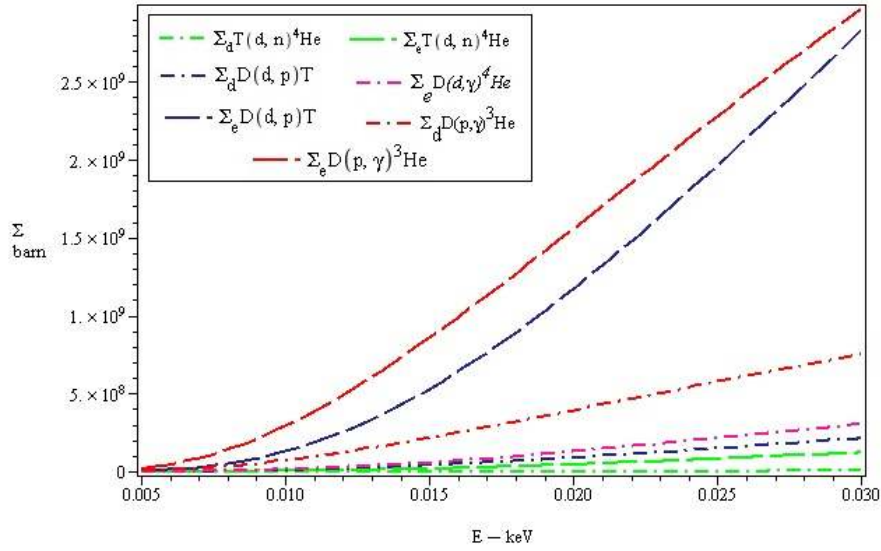


Figure 8: The two dimensional seven maximum macroscopic cross sections as a function of the incoming particle energy for different host particles and different reactions. The maximum cross sections belong to electron and deuteron host particles. The best reactions are the $D(p, \gamma)^3\text{He}$ and $D(d, p)T$.

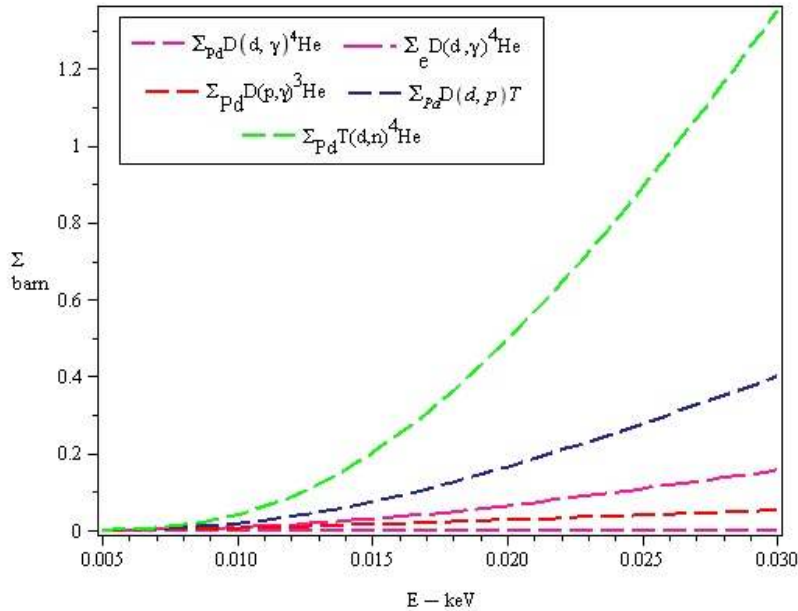


Figure 9: The two dimensional five minimum macroscopic cross sections as a function of the incoming particle energy for different host particles and different reactions. The maximum cross section belongs to palladium host particle for $T(d, n)^4\text{He}$ and $D(d, p)T$.

Figs. 6 to 9 emphasize that the electron and deuteron host particles represent the maximum cross sections. Among of all reactions $D(d, p)T$ is the best reaction because it has a maximum cross section, but the numerical difference between $D(d, p)T$ and $T(d, n)^4\text{He}$ is low.

Now for comparison the ordinary and macroscopic FCS with regard LEISSIC, we plotted Figs. 10,11,12 and 13. In this case, green, dark blue and red colors indicate the cross section of electron, deuteron and Pd as a host particles selection respectively. The light blue implies ordinary FCS.

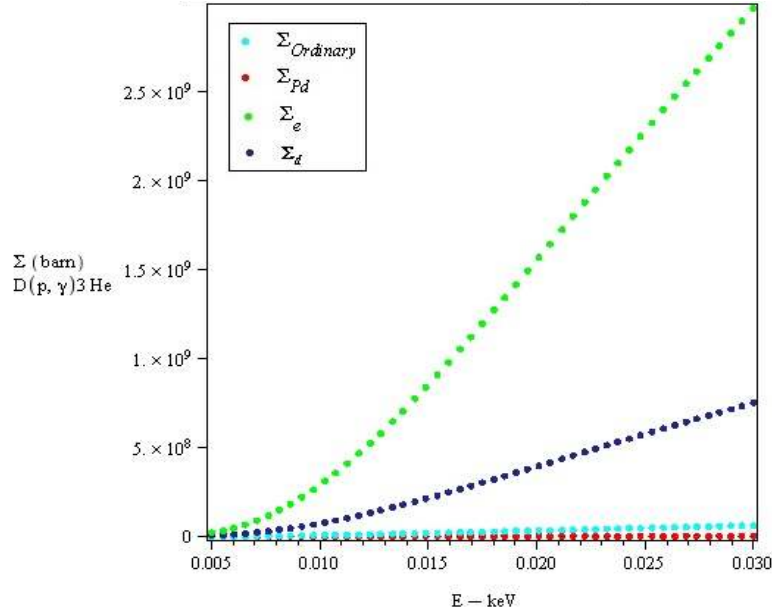


Figure 10: The macroscopic cross section for $D(p,\gamma)^3\text{He}$ reaction with regarding different host particles and ordinary state in terms of incoming particle energy. It shows the comparison of the cross section of LEISSIC with an ordinary cross section for the $D(p,\gamma)^3\text{He}$ reaction. The only graph that is lower than ordinary state is the palladium graph.

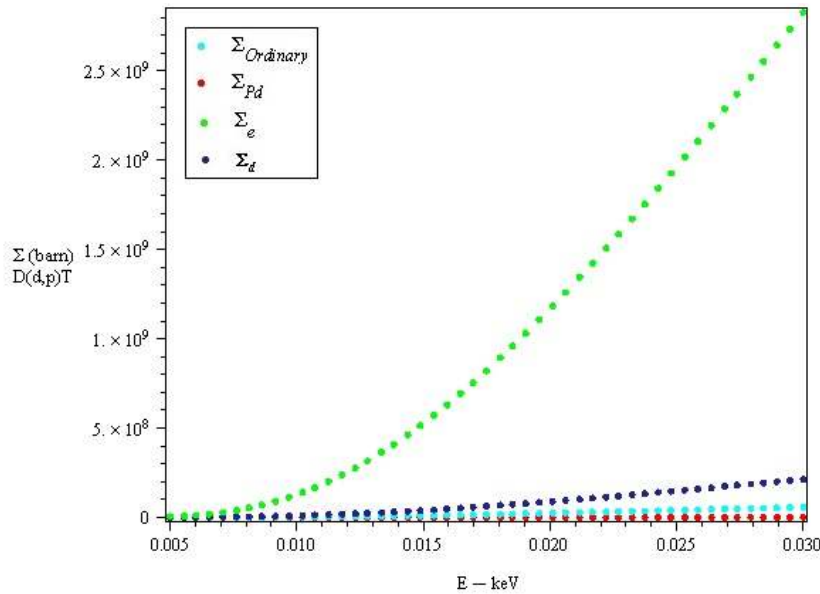


Figure 11: The macroscopic cross section for $D(d,p)T$ reaction with regard different host particles and ordinary state in terms of incoming particle energy. It shows the comparison of the cross section of LEISSIC with an ordinary cross section for $D(d,p)T$ reaction. The only graph that is lower than ordinary state is the palladium graph.

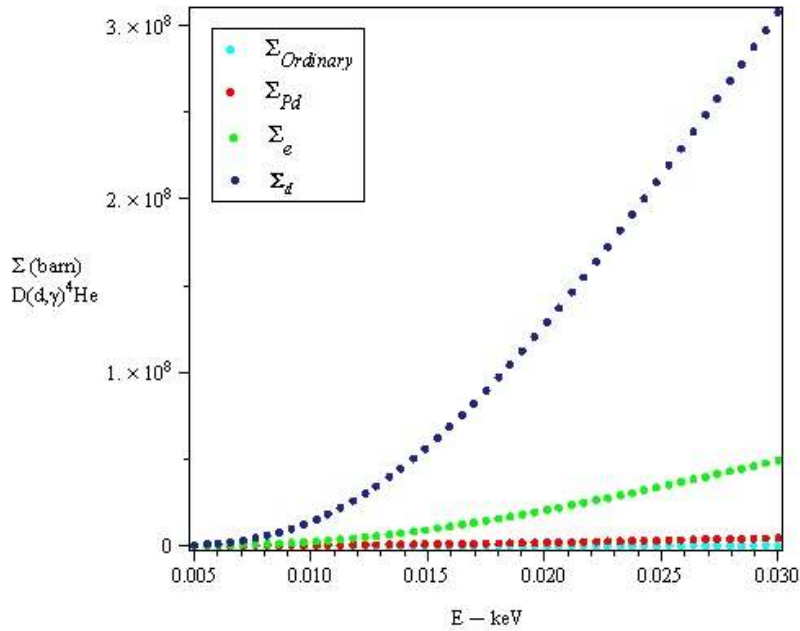


Figure 12: The macroscopic cross section for $D(d,\gamma)^4\text{He}$ reaction with regarding different host particles and ordinary state in terms of incoming particle energy. It shows the comparison of the cross section of LEISSIC with an ordinary cross section for the $D(d,\gamma)^4\text{He}$ reaction. The only graph that is lower than ordinary state is the palladium graph

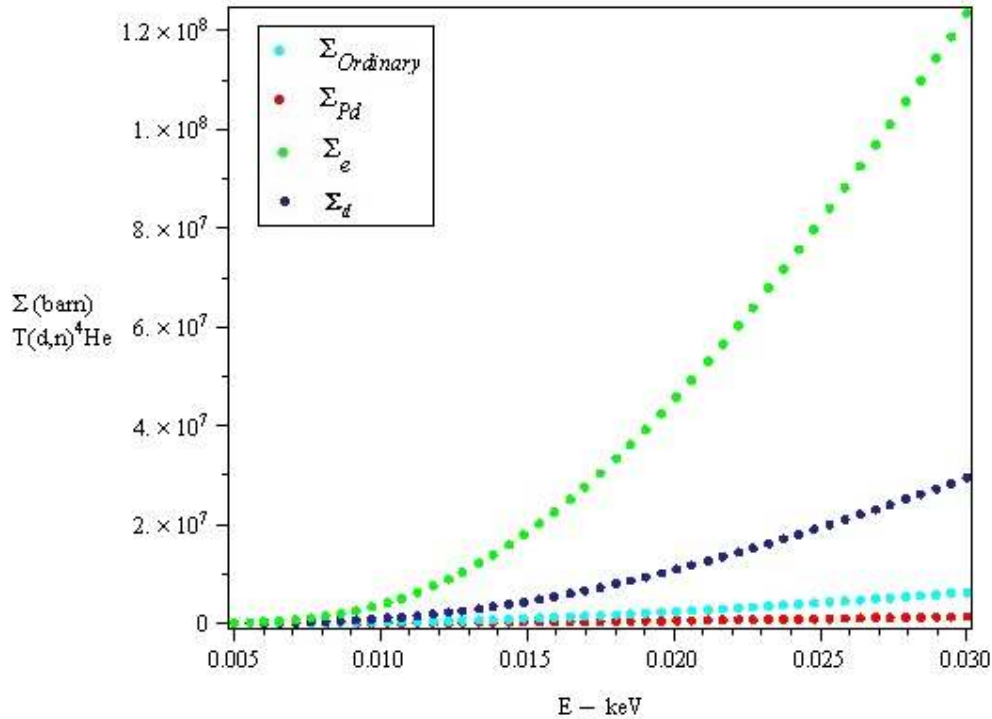


Figure 13: The macroscopic cross section for $T(d,n)^4\text{He}$ reaction with regard different host particles and an ordinary state in terms of incoming particle energy. It shows the comparison of the cross section of LEISSIC with an ordinary cross section for $T(d,n)^4\text{He}$ reaction. The only graph that is lower than ordinary state is the palladium graph

For comparing different host particle cross section such as $D(p,\gamma)^3\text{He}$, $D(d,p)\text{T}$ and $T(d,n)^4\text{He}$, we have $\Sigma_e > \Sigma_d > \Sigma_{pd}$ but just for $D(d,\gamma)^4\text{He}$ $\Sigma_d > \Sigma_e > \Sigma_{pd}$. Also, from comparing different host

particle cross section with the ordinary cross section, we have $\Sigma_e > \Sigma_d > \Sigma_{ordinary} > \Sigma_{pd}$ for all kinds of reactions except $D(d,\gamma)^4\text{He}$. By comparing LEISSIC and ordinary cross sections, we distinguish that the ordinary cross section is minimized. As the results show, graphs verify the theory that expresses “there is a magnificent enhancement in cross section when we consider lattice effect in solid state internal conversion in our calculations”.

7. Deliberations of the solidstate internal conversion coefficient for different fusion reactions in Palladium crystal environment

With regard to the definition that exists in Ref. 20, we can write $v_{eff} = A\Delta R_h$, where A is the cross section of the beam, ΔR_h is the “differential” range, which is, the distance within the energy of the incoming particle can be considered unchanged. The $\Delta R_h \ll R_h$ condition helps in an order of magnitude estimate of ΔR_h , where R_h is the stopping range of a proton which is about $8 \times 10^{-2} \mu\text{m}$ at $E = 0.01 \text{ MeV}$ in Pd [28]. The quantities A and R_h were measured in mm^2 and $10^{-3} \mu\text{m}$ units. The solid state internal conversion coefficient is introduced as,

$$\alpha_{SSIC} = A\Delta R_h C_1 / S(0) \quad (29)$$

By using the amounts exist in tables 1, 3 and replacing them inside Eq.29 the solid state internal conversion coefficient for different reactions can be found. This coefficient represents the internal conversion rate in different reactions. The results of our calculations are summarized in table 5.

Table 5: The values of solid state internal conversion coefficient in different reactions for e, 4d and d channels

Type of reactions	$\alpha_{SSIC,d} A\Delta R_h$	$\alpha_{SSIC,e,4d} A\Delta R_h$
$D(p,\gamma)^3\text{He}$	$u \times 7.8 \times 10^5$	3.1×10^9
$D(d,p)\text{T}$	$u \times 3.03 \times 10^4$	3.2×10^6
$D(d,\gamma)^4\text{He}$	$u \times 3.398 \times 10^2$	5.42×10^{-20}
$T(d,n)^4\text{He}$	$u \times 0.03$	12.7

We plainly find out from this table that solid state internal conversion more occurs in $D(p,\gamma)^3\text{He}$ and $D(d,p)\text{T}$ reactions.

8. Conclusion

By brushing up all of our computations, we realize that the lattice effect in solid state internal conversion cross section is more than an ordinary state for each reaction. In previous experiments the complete reason for increasing cross section experimentally for these reactions are not explained, but in this work by analyzing LEISSIC we can justify those observations theoretically. Our theoretical studies prove that the results of the experiments are given in below.

Whenever we consider the crystalline lattice in our calculations, since deuterium and the other fusible particles are solved inside a lattice as a sublattice, the required energy for locating these

particles in a regular shape in the lattice reduces the Coulomb barrier more than before and increases the probability of fusion reaction. Thus, when fusion reactions take place in the crystalline solid state environment the effect of lattice in solid state internal conversion processes cannot be ignored.

From graphs and internal conversion mechanism, we understand **thatsince** the internal conversion rates of $D(p,\gamma)^3\text{He}$ and $D(d,p)\text{T}$ reactions are more than others, they are the best choices to study.

9. References

[1] T. Graham, *Collected Chemical and Physical Researches*, Ed. R. Angus Smith, Edinburgh, 1987.

[2] M. Fleischmann and S. Pons, *J. Electroanal. Chem.* **261**, 301, 1989.

[3]“Low Energy Nuclear Reactions-Chimically Assisted Nuclear Reactions.”, <http://WWW.lenr-canr.org/>(accessed February 13, 2004)

[4] Mallove, E., *Fire From Ice.*, John Wiley, pp. 246-248 (1991)

[5]F. A. Paneth and K. Peters; Review of article, published in *Nature*, May 14 (1927)

[6] G. Taubes, *Bad Science: The Short Life and Weird Times of Cold Fusion*. New York: Random Hous, 1993, p. 424.

[7]Huizenga, J. R., *Cold Fusion: The Scientific Fiasco of The Century* (Oxford University Press, Oxford, New York) pp. 184(1993)

[8]G. Taubes, *Bad Science: The Short Life and Weird Times of Cold Fusion*. New York: Random Hous, 1993, pp. 136–138.

.....

[9] P. Kalman and T. Keszthelyi, *Phys. Rev. C* **69**, 031606(R) (2004).

[10]C. Rolfs and E. Somorjai, *Nucl. Instrum. Methods B* **99**, 297 (1995).

[11]J.P. Biberian, *Int. J. Nuclear Energy Science and Technology* 3(2007)31-43
"Condensed Matter Nuclear Science (Cold Fusion) an update".

[12] K. Czernski, A. Huke, P. Heide, M. Hoefft, and G. Ruprecht in *Nuclei in the Cosmos V, Proceedings of the International Symposium on Nuclear Astrophysics*, edited by N. Prantzos and S. Harissopulos (Editions Frontieres, Volos, Greece, 1998) p. 152.

[13] K. Czernski, A. Huke, A. Biller, P. Heide, M. Hoefft, and G. Ruprecht, *Europhys. Lett.* **54**, 449 (2001).

[14]A. Huke, *Die Deuteronen-fusionsreaktionen in Metallen*, PhD Thesis, Technische Universität, Berlin, (2002).

- [15] F. Raiola *et al.*, Eur. Phys. J. A **13**, 377(2002); Phys. Lett. **547**, 193 (2002).
- [16] C. Bonomo *et al.*, Nucl. Phys. **A719**, 37c (2003).
- [17] J. Kasagiet *al.*, J. Phys. Soc. Jpn. **71**, 2881 (2002).
- [18] K. Czerniet *al.*, Eurouphys. Lett. **54**, 449 (2001); Nucl. Instrum. Methods Phys. B **193**, 183 (2002).
- [19] A. Huke, K. Czerniet, and P. Heide, Nucl. Phys. **A719**, 279c (2003).
- [20] P. Kalman and T. Keszthelyi, Phys. Rev. C **79**, 031602(R) (2009).
- [21] Y. Arata and Y. C. Zhang: Proc. Jpn. Acad. B, **70** (1994) 106; **71** (1995) 304; Jpn. J. Appl. Phys., **37** (1998) L1274; **38** (1999) L774.
- [22] Y. Arata and Y. C. Zhang: *Proc. Jpn Acad. B*, **78** (2002) 57.
- [23] Y. Arata and Y. C. Zhang: *J. High Temp. Soc. Jpn.* **29** (Special Vol.) (2008), 1-44; ICCF10.
- [24] C. Angulo *et al.*, Nucl. Phys. **A656**, 3 (1999).
- [25] J. M. Ziman, Principles of the Theory of Solids (Cambridge University Press, Cambridge, 1964), pp. 148-150 .
- [26] C. Cohen-Tannoudji, B. Diu, and F. Laloë, Quantum Mechanics, Vol. 1 (Wiley, New York [English version]/Hermann, Paris, 1977).
- [27] K. Alder *et al.*, Rev. Mod. Phys. **28**, 432 (1956).
- [28] R. B. Firestone and V. S. Shirley, Tables of Isotopes, 8th ed. (wiley, New York, 1996).
- [29] S. Krivit and B. Davi, New Scientist: Extraordinary Evidence, 29 March 2003.